

Carrier mobility degradation in metaloxide semiconductor field effect transistors due to oxide charge

A. Phanse, D. Sharma, A. Mallik, and J. Vasi

Citation: *Journal of Applied Physics* **74**, 757 (1993); doi: 10.1063/1.355249

View online: <http://dx.doi.org/10.1063/1.355249>

View Table of Contents: <http://scitation.aip.org/content/aip/journal/jap/74/1?ver=pdfcov>

Published by the [AIP Publishing](#)

Articles you may be interested in

[The channel mobility degradation in a nanoscale metal–oxide–semiconductor field effect transistor due to injection from the ballistic contacts](#)

J. Appl. Phys. **109**, 056103 (2011); 10.1063/1.3554623

[On resolving hot carrier induced degradation mechanisms in silicon on sapphire metaloxide semiconductor field effect transistors](#)

Appl. Phys. Lett. **63**, 1912 (1993); 10.1063/1.110646

[Metaloxide semiconductor field effect transistor characteristics as influenced by carrier mobility variation along the channel](#)

J. Appl. Phys. **72**, 3606 (1992); 10.1063/1.352301

[Hot carrier induced degradation of metaloxide semiconductor field effect transistors: Oxide charge versus interface traps](#)

J. Appl. Phys. **65**, 354 (1989); 10.1063/1.342548

[Effect of oxide field on hot carrier induced degradation of metaloxide semiconductor field effect transistors](#)

Appl. Phys. Lett. **50**, 1188 (1987); 10.1063/1.97906

An advertisement for Asylum Research Cypher AFMs. The background is dark blue with a film strip graphic on the left. The text is in white and orange. The Oxford Instruments logo is in the bottom right corner.

Not all AFMs are created equal
Asylum Research Cypher™ AFMs
There's no other AFM like Cypher

www.AsylumResearch.com/NoOtherAFMLikeIt

OXFORD
INSTRUMENTS
The Business of Science®

Carrier mobility degradation in metal-oxide-semiconductor field-effect transistors due to oxide charge

A. Phanse, D. Sharma, A. Mallik, and J. Vasi

Department of Electrical Engineering, Indian Institute of Technology, Bombay 400 076, India

(Received 16 November 1992; accepted for publication 22 March 1993)

Radiation causes oxide charge buildup which can degrade carrier mobility in the inversion layer of a metal-oxide-semiconductor field-effect transistor (MOSFET). An expression for the carrier mobility in MOSFETs due to oxide charge scattering has been derived. The model predicts the mobility degradation given any specified charge density profile in the oxide. It accounts for screening of oxide charges by channel carriers. To validate the proposed model we performed an experiment to place a measured quantity of charge at a definite position in the gate oxide and then measured the mobility degradation. The experimental results are in good agreement with the predictions of the model.

Radiation causes oxide charge buildup and interface-state generation in metal-oxide-semiconductor field-effect transistors (MOSFETs). Though it is well recognized that the generation of interface states is the dominant mobility degradation mechanism, radiation-induced trapped charge can also degrade mobility significantly¹⁻⁶ and therefore cannot be neglected. Mobility degradation due to surface oxide charges has been modeled previously,^{7,8} and this model has also been used for mobility degradation due to interface states.⁹⁻¹¹ However, since radiation-induced oxide charges reside in the bulk of the oxide, they will degrade mobility of carriers differently as compared to surface charges. In this paper we present a model for mobility degradation due to scattering from bulk oxide charges. The model calculates mobility for any charge density profile along the depth of the oxide. The screening of the oxide charges by channel carriers has been taken care of in the model. The model has no adjustable parameters. We present experimental data which show excellent agreement with the model.

We model the oxide charge as a collection of positive charges having a known distribution in the volume of the oxide. We construct a box having dimensions $2h$, $2h$, Z_{inv} (Fig. 1) in the inversion layer below a unit charge in the oxide such that a carrier in the box is scattered by only the single oxide charge above the box. We therefore fix the dimension h of the box such that

$$\left(\int_0^{t_{\text{ox}}} N(x,y,z) dz \right) 2h2h = 1,$$

where $N(x,y,z)$ is the oxide charge density distribution (cm^{-3}) and t_{ox} is the thickness of the oxide.

The inversion layer thickness is $Z_{\text{inv}} = Z_{\text{CL}} + Z_{\text{QM}}$ (Ref. 12), where Z_{CL} is the classical inversion layer thickness and Z_{QM} is the quantum mechanical 0 K inversion layer thickness. Notice that the dimensions of a box in the inversion layer are decided by the oxide charge density, the perpendicular electric field, and the electron temperature.

We assume that a carrier in the box is scattered by only the single oxide charge above the box and therefore its

trajectory is a parabola. Using the Rutherford scattering law¹³ we calculate the minimum and maximum angles (θ_{min} and θ_{max}) through which a carrier can be scattered by an oxide charge q at a distance z above the interface.

$$\tan(\theta/2) = R/b,$$

$$R = \frac{q^2}{4\pi\epsilon_s m^* v^2},$$

where ϵ_s is the silicon permittivity, m^* is the effective mass of the carrier, and v is the carrier velocity. Using the property of the parabolic path, we express the impact parameter for an electron scattered by an oxide charge as $b = \sqrt{d^2 + 2dR}$, where d is the closest distance from an oxide charge that the electron can approach in its trajectory in a box in the inversion layer. The scattering cross section of an oxide charge is calculated by integrating between the possible angles of scattering:¹⁴

$$\sigma_c = 2\pi \int_{\theta_{\text{min}}}^{\theta_{\text{max}}} (1 - \cos\theta) \frac{1}{4} R^2 \text{cosec}^4 \frac{\theta}{2} \sin\theta d\theta.$$

The average scattering cross section ($\sigma_{c_{\text{av}}}$) for a given oxide charge distribution is calculated by averaging over the cross sections of all the unit charges in the gate oxide.

The channel carriers can screen the oxide charge. At high gate fields the carrier density is high and the oxide charges are screened effectively. We use the simple screening approximation¹² $\sigma_{c_{\text{eff}}} = \sigma_{c_{\text{av}}} C_0 n_I^{-1/4}$, where n_I is the average carrier density (m^{-3}) in the inversion layer. When the channel is weakly inverted the carrier density is very small and there is negligible screening. Therefore the constant of proportionality C_0 is fixed by making $[C_0 n_I^{-1/4}]_{E_p=0.01 \text{ MV/cm}} = 1$. The weak inversion perpendicular field E_p was chosen to be 0.01 MV/cm to make the weak inversion layer thickness consistent with Ref. 15.

The relaxation time between two scattering events due to oxide charges having a uniform charge distribution in the x and y (lateral) directions is given by

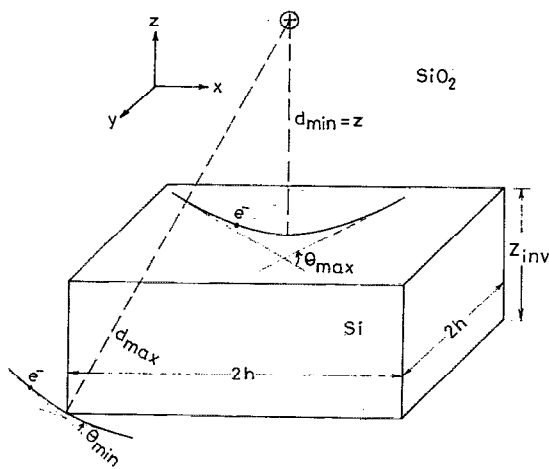


FIG. 1. Construction of a box in the MOSFET inversion layer.

$$\tau = \frac{1}{\left[\int_0^{z_{ox}} N(z) dz / Z_{inv} \right] \sigma_{c,eff} \nu}$$

where $\frac{1}{2} m^* v^2 = \frac{3}{2} kT = E$. For spherical energy bands the average relaxation time $\langle |\tau| \rangle$ can be calculated as in Ref. 14, and the oxide charge scattering electron mobility ($\mu_{ox} = q \langle |\tau| \rangle / m^*$) is then given by

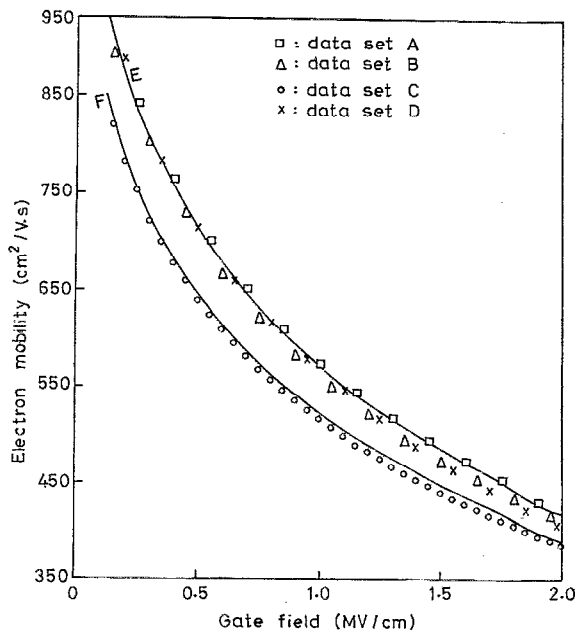


FIG. 2. Effective electron mobility as a function of gate bias. *A*, initial mobility; *B*, $3.5 \times 10^{11} \text{ cm}^{-2}$ atoms of sodium are introduced into the gate oxide and pulled up to the gate-SiO₂ interface; *C*, charge pushed down to the Si-SiO₂ interface; *D*, charge pulled up once again to the gate-SiO₂ interface; *E*, model curve when the charge has a Gaussian profile with its peak 20 Å from the gate-SiO₂ interface and falling to 0.1 of its peak value 30 Å from the peak; *F*, model curve when the charge is peaked 20 Å from the Si-SiO₂ interface.

$$\mu_{ox} = \frac{32\pi^{1/2} \epsilon_{Si}^2 (2kT)^{3/2} Z_{inv}}{C_0 n_I^{-1/4} q^3 m^{*1/2} \int_0^{z_{ox}} N(z) g(z) dz}$$

where $g(z)$ is a weak function of energy E :

$$g(z) = \ln \left(\frac{R + \sqrt{(Z_{inv} + z)^2 + 2h^2}}{R + z} \right)$$

To validate the proposed model we need to do a controlled experiment in which we know the charge distribution in the oxide. It is difficult to find the exact distribution of the oxide charge introduced due to radiation. We decided to simulate radiation-induced oxide charge by purposely introducing sodium into the gate oxide of the transistor. Sodium has a high mobility in SiO₂ and can be moved within the gate oxide by subjecting the transistors to a bias-temperature stress. The quantity of sodium introduced can be accurately measured from the shift in threshold voltage when the sodium atoms are situated at the two extreme positions in the gate oxide.

The test transistors were fabricated using a standard silicon gate NMOS process and had a gate oxide of 400 Å. Sodium was introduced by exposing the transistors to an aqueous solution of sodium hypophosphite. A field of $\pm 1.5 \text{ MV/cm}$ and a temperature stress of 250 °C were used to move the sodium atoms. Mobility was found by measuring the ac channel conductance after superimposing a 500 Hz, 20 mV rms ac voltage on a 40 mV dc voltage at the drain. The threshold voltage was calculated from the intersection with the V_G axis of the tangent to the linear I_D - V_G curve ($V_D = 0.1 \text{ V}$) at the point of inflexion.

In Fig. 2, data set *A* shows the mobility as a function of

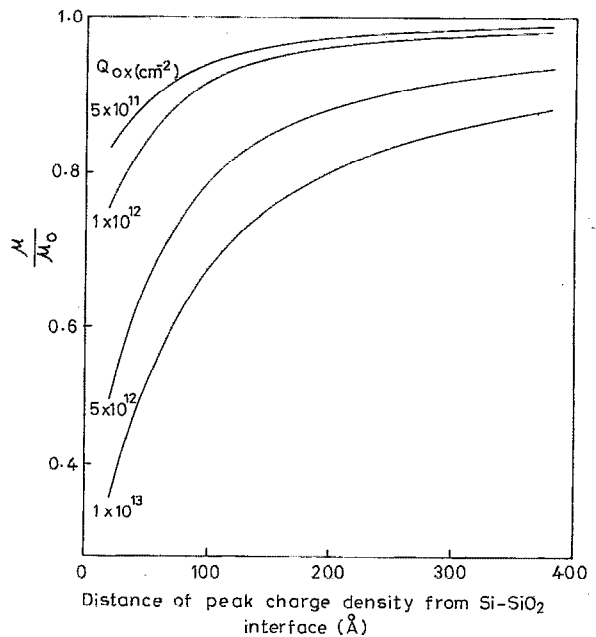


FIG. 3. The mobility predictions of the model vs the position of the centroid of charge in the oxide for different amount of charge. The charge is a Gaussian distribution falling to 0.1 of its peak value 30 Å from the peak.

gate bias before introduction of sodium. Sodium was introduced and pulled up to the gate (data set *B*), then pushed down to the Si interface (data set *C*), and again pulled up to the gate (data set *D*). Recovery of the mobility to its initial value indicates that the observed mobility degradation is due to the change in position of oxide charge and not due to other effects such as generation of interface states.

The amount of sodium introduced was found to be $3.5 \times 10^{11} \text{ cm}^{-2}$. After each bias-temperature stress the sodium is located at either interface. The oxide charge density is modeled as a Gaussian profile with its peak 20 Å from the interface and falling to 0.1 of its peak value 30 Å from the peak. The theoretical mobility curves are obtained using $\mu^{-1} = \mu_{\text{initial}}^{-1} + \mu_{\text{ox}}^{-1}$ where μ_{initial} is the mobility measured before the introduction of sodium. The model predicts the theoretical mobility curves *E* and *F* (Fig. 2) when the sodium atoms are located at either interface and have the Gaussian profile described earlier. The model does not use any adjustable parameters and fits the experimental results very well. This experiment was repeated for different quantities of introduced charge and the model continues to be a good fit to experiment. The fit of the model to experiment is not very sensitive to the exact choice of the charge density profile in the oxide.

Having validated the model for the extreme cases, we can predict the dependence of mobility for different oxide charge distributions. The mobility predictions of the model versus the position of the centroid of charge in the oxide for different amount of charge are plotted in Fig. 3. We see that the oxide charges situated at a distance of several hundred angstroms from the interface also degrade mobility significantly. This is in contrast with the common belief

that only charge close to the interface is important for mobility degradation.

In summary, we presented a model which determines the oxide charge scattering mobility given the charge density distribution in the oxide. The model is a good fit to experiment, and shows that oxide charge relatively deep in the oxide can also degrade mobility.

This work was funded by the Department of Electronics, Government of India.

- ¹D. Zupac, K. F. Galloway, R. D. Schrimpf, and P. Augier, *Appl. Phys. Lett.* **60**, 3156 (1992).
- ²S. Dimitrijević, S. Golubović, D. Zupac, M. Pejović, and N. Stojadinović, *Solid-State Electron.* **32**, 349 (1989).
- ³S. Dimitrijević and N. Stojadinović, *Solid-State Electron.* **30**, 991 (1987).
- ⁴F. B. McLean and H. E. Boesch, Jr., *IEEE Trans. Nucl. Sci.* **NS-36**, 1772 (1989).
- ⁵N. S. Saks, K. B. Klein, and D. L. Griscom, *IEEE Trans. Nucl. Sci.* **NS-35**, 1234 (1988).
- ⁶C. L. Wilson and J. L. Blue, *IEEE Trans. Nucl. Sci.* **NS-31**, 1448 (1984).
- ⁷S. C. Sun and J. D. Plummer, *IEEE Trans. Electron Devices* **ED-27**, 1497 (1980).
- ⁸C. T. Sah, T. H. Ning, and L. L. Tschoop, *Surf. Sci.* **32**, 561 (1972).
- ⁹F. C. Hsu and S. Tam, *IEEE Electron Device Lett.* **EDL-5**, 50 (1984).
- ¹⁰K. F. Galloway, M. Gaitan, and T. J. Russel, *IEEE Trans. Nucl. Sci.* **NS-31**, 1497 (1984).
- ¹¹F. W. Sexton and J. R. Schwank, *IEEE Trans. Nucl. Sci.* **NS-32**, 3975 (1985).
- ¹²S. A. Schwarz and S. E. Russek, *IEEE Trans. Electron Devices* **ED-30**, 1634 (1983).
- ¹³M. Born and R. J. Blin-Stoyle, *Atomic Physics*, 7th ed. (Blackie & Son, Glasgow, 1962), p. 343.
- ¹⁴R. A. Smith, *Semiconductors*, 2nd ed. (Cambridge University, Cambridge, 1978), pp. 100 and 117.
- ¹⁵A. P. Gnädinger and H. E. Talley, *Solid-State Electron.* **13**, 1301 (1970).